

Biochemical Characterization of MmoS, a Sensor Protein Involved in Copper-Dependent Regulation of Soluble Methane Monooxygenase[†]

Uchechi E. Ukaegbu, Shannon Henery, and Amy C. Rosenzweig*

Department of Biochemistry, Molecular Biology, and Cell Biology and Department of Chemistry, Northwestern University, Evanston, Illinois 60208

Received April 10, 2006; Revised Manuscript Received June 6, 2006

ABSTRACT: Methane monooxygenase (MMO) enzymes catalyze the oxidation of methane to methanol in methanotrophic bacteria. Several strains of methanotrophs, including *Methylococcus capsulatus* (Bath), express a membrane-bound or particulate MMO (pMMO) at high copper-to-biomass ratios and a soluble MMO (sMMO) form when copper is limited. The mechanism of this “copper switch” is not understood. The *mmoS* gene, located downstream of the sMMO operon, encodes a sensor protein that is part of a two-component signaling system and has been proposed to play a role in the copper switch. MmoS from *M. capsulatus* (Bath) has been cloned, expressed, and purified. The purified protein is a tetramer of molecular mass 480 kDa. Optical spectra indicate that MmoS contains a flavin cofactor, identified as flavin adenine dinucleotide (FAD) by fluorescence spectroscopy and chromatographic analysis. The redox potential of the MmoS-bound FAD, which binds within the N-terminal PAS–PAC domains, is -290 ± 2 mV at pH 8.0 and 25 °C. Despite extensive efforts, MmoS could not be loaded with Cu^I or Cu^{II}, indicating that MmoS does not sense copper directly. These data suggest that MmoS functions as a redox sensor and provide new insight into the copper-mediated regulation of sMMO expression.

Methanotrophs are a subset of methylotrophic bacteria, aerobic organisms that grow on one-carbon compounds such as methanol, methane, methylated amines, and halomethanes. Methanotrophs are unique in their ability to use methane as their sole source of carbon and energy and play a key role in mitigating the effects of methane on global warming (1). The first step in methane metabolism is the oxidation of methane to methanol by methane monooxygenase (MMO)¹ enzyme systems (2, 3). Several strains of methanotrophs, including *Methylococcus capsulatus* (Bath), can express two forms of the enzyme depending upon copper availability. At high copper levels ($\sim 4 \mu\text{M}$), a membrane-bound or particulate MMO (pMMO) is expressed, whereas at low copper-to-biomass ratios ($< 0.8 \mu\text{M}$), a soluble MMO (sMMO) is produced (4–6). The mechanism of this “copper switch” has not been elucidated. sMMO has a broader substrate specificity than pMMO (7, 8) and is therefore more versatile for bioremediation applications. pMMO is prevalent at the high copper concentrations typical of polluted environments, however (9). Understanding the copper switch mechanism could aid in engineering methanotrophic bacteria to express sMMO at high copper levels.

Sequencing and mutagenesis studies suggest that *M. capsulatus* (Bath) sMMO is regulated by four genes located downstream of the sMMO operon, *mmoR*, *mmoG*, *mmoS*,

and *mmoQ* (10). The proteins encoded by these genes have not been characterized biochemically. MmoR is hypothesized to be a σ^N -dependent transcriptional activator when copper levels are low (10). Mutation of this gene in both *M. capsulatus* (Bath) (10) and a related organism, *Methylosinus trichosporium* OB3b (11), abolishes sMMO expression. The *mmoG* gene encodes a GroEL-like protein that is also essential for sMMO expression and might participate in the proper folding and assembly of MmoR or the sMMO complex (10, 11). The polypeptides encoded by *mmoS* and *mmoQ* are sequentially similar to two-component signaling systems (12, 13). In these systems, the first component detects environmental stimuli via its sensor domain and autophosphorylates a specific histidine residue within its histidine kinase domain. The phosphoryl group is then transferred to an aspartic acid residue in the second component, a response regulator protein, activating an effector domain. On the basis of sequence comparisons, MmoS corresponds to the sensor protein and MmoQ resembles the regulator protein. Well-studied examples of two-component systems include NifL and NifA, which regulate nitrogenase expression (14), and CheA and CheY of the *Escherichia coli* chemotaxis system (15).

Analysis of the MmoS sequence using the simple modular architecture research tool (SMART) (16) indicates the presence of multiple domains (Figure 1). An N-terminal transmembrane domain is followed by two predicted PAS–PAC domains (17, 18) and a GAF domain (19). PAS–PAC signaling modules respond to changes in the redox potential, light, concentrations of small ligands, and overall energy level of the cell. Many PAS domains detect stimuli via associated cofactors including heme, flavin adenine dinucle-

[†] This work was supported by National Institutes of Health Grant GM70473. U.E.U. was supported in part by National Institutes of Health Training Grant GM8061.

* To whom correspondence should be addressed. Telephone: 847-467-5301. Fax: 847-467-6489. E-mail: amyr@northwestern.edu.

¹ Abbreviations: MMO, methane monooxygenase; pMMO, particulate methane monooxygenase; sMMO, soluble methane monooxygenase; FAD, flavin adenine dinucleotide.

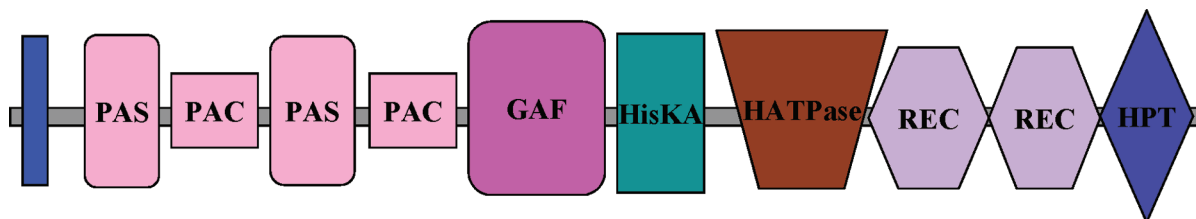


FIGURE 1: Predicted domain organization of MmoS.

otide (FAD), and chromophores, such as 4-hydroxycinnamic acid (18). These domains in MmoS have been proposed to play a role in the copper switch, either through another protein or by binding copper ions directly (10). Although canonical copper-binding motifs are not present, the GAF domain contains an MXXCXC sequence that could potentially bind metal ions. In response to the copper signal, the C-terminal HATPase domain likely catalyzes the ATP-dependent phosphorylation of a histidine residue in the HisKA domain (Figure 1). The two receiver domains (REC) and the His-containing phosphotransfer domain (HPT) are hypothesized to mediate phosphotransfer to MmoQ, the regulator protein, which in turn may signal MmoR to activate the transcription of the sMMO operon (10). As a first step toward investigating the role of MmoS in the copper switch mechanism, we have cloned, expressed, and purified *M. capsulatus* (Bath) MmoS lacking the N-terminal transmembrane domain. Here, we report the biochemical characterization of MmoS, including its oligomerization state, copper-binding properties, and the identification and redox-potential determination of a FAD cofactor.

MATERIALS AND METHODS

Expression and Purification of MmoS. The *mmoS* gene lacking the N-terminal transmembrane domain (residues 85–1178) was amplified with Pfx polymerase (Invitrogen) from *M. capsulatus* (Bath) genomic DNA using the following primers: forward, 5'-GACGACGACAAGATGCAGCGCAACAAGAGCTCCTGGACGCCC-3', and reverse, 5'-GAGGAGAAGCCCGGTTTCATTGCGCAGCATCGTTCGTGCCCT-3'. Using the Ek/LIC cloning kit (Novagen), the *mmoS* gene was inserted into the plasmid pET46a, which includes an N-terminal (His)₆ tag with an adjacent enterokinase cleavage site. B834(DE3)pLysS *E. coli* cells (60 mL cultures) transformed with the plasmid were grown for 16 h in Terrific Broth and then scaled up to 1 L. Chloramphenicol and carbenicillin were added to final concentrations of 34 and 100 μ g/mL, respectively. To induce protein expression, isopropyl- β -D-thiogalactopyranoside (IPTG) was added to a final concentration of 0.5 mM at an OD₆₀₀ of 0.9–1.0 and the cells were grown for 3–4 h at 37 °C. To investigate copper binding, the growth medium was supplemented with 400 μ M CuCl₂ and 400 μ M CuSO₄ at induction in separate experiments. Cells were harvested by centrifugation at 5000g for 10 min at 4 °C. For lysis, the cell pellets were resuspended in 50 mM Tris (pH 8.0) with 0.1% Triton X-100, and phenylmethylsulfonyl fluoride (PMSF) was added to a final concentration of 1 mM. The cell suspension was frozen at –20 °C and lysed by thawing in lukewarm water.

The crude cell extract was obtained by ultracentrifugation at 163000g for 1 h. All purification steps were performed at 4 °C. MmoS was purified initially by nickel-affinity chromatography on a chelating Sepharose column equilibrated with 50 mM Tris (pH 8.0), 0.5 M NaCl, and 10% glycerol (buffer A). Approximately 250 mL of crude cell extract was loaded onto the column, which was washed with 15% 50 mM Tris (pH 8.0), 0.5 M NaCl, 10% glycerol, and 0.5 M imidazole (buffer B). MmoS eluted at 35% buffer B (175 mM imidazole). Fractions containing MmoS by sodium dodecyl sulfate–polyacrylamide gel electrophoresis (SDS–PAGE) were pooled and concentrated using YM-30 centripres (Amicon). The concentrated protein was purified further by gel-filtration chromatography on a Superdex 200 column equilibrated with buffer A. After removal of NaCl by dialysis, the (His)₆ tag was cleaved by the addition of 0.1 unit/ μ L enterokinase (Novagen) per 3.2 mg of purified protein and was separated by nickel-affinity chromatography.

The MmoS sensor domain, consisting of the two PAS–PAC domains and the GAF domain (residues 85–508), was also amplified with Pfx polymerase (Invitrogen) from *M. capsulatus* (Bath) genomic DNA using the following primers: forward, 5'-GACGACGACAAGATGCAGCGCAACAAGAGCTCCTGGACGCCC-3', and reverse, 5'-GAGGAGAAGCCCGGTTTCATTGCGCAGCATCGTTCGTGCCCT-3'. The gene was inserted into the plasmid pET32Ek/LIC, which includes an N-terminal Trx-S-(His)₆ tag with an adjacent enterokinase cleavage site. Cultures (50 mL) of Rosetta-gami(DE3)pLysS *E. coli* cells transformed with the plasmid were grown overnight in Luria Bertani media and then scaled up to 1 L. Chloramphenicol and carbenicillin were added to final concentrations of 34 and 100 μ g/mL, respectively. IPTG was added to a final concentration of 0.5 mM at an OD₆₀₀ of 0.7–0.9, and the cells were incubated for 3–4 h at 37 °C. Cells were lysed; the crude extract was prepared; and the sensor domain was purified by nickel-affinity chromatography as described above.

Molecular-Mass Determination. The molecular mass of MmoS was determined on a Sephacryl-300 (S-300) gel-filtration column. To measure the void volume, a fresh solution of Blue Dextran 2000 (1.0 mg/mL) was prepared in buffer A and applied to the column. The following molecular-mass standards (Amersham) were used to calibrate the column: thyroglobulin, 669 kDa; ferritin, 440 kDa; catalase, 232 kDa; aldolase, 158 kDa; albumin, 67 kDa; and ovalbumin, 43 kDa. K_{av} values for each protein were calculated on the basis of the equation $K_{av} = V_e - V_o/V_t - V_o$, in which V_e is the elution volume of the protein, V_o is the void volume, and V_t is the total bed volume. The K_{av} value for each protein standard was plotted against its molecular weight on the logarithmic scale, and the molecular

mass of MmoS was calculated using its elution volume and this plot.

Copper-Binding Studies. Purified MmoS solutions (85 and 200 μM), with and without the (His)₆ tag, were dialyzed overnight at 4 °C with one buffer change against 500 mL of 50 mM Tris (pH 7.2, 7.4, or 8.0), 100 mM NaCl, 1 mM ethylenediaminetetraacetic acid (EDTA), 10 mM dithiothreitol (DTT), and 5% glycerol to remove any nonspecifically bound metal ions. The protein samples were then dialyzed into the same buffer without EDTA and DTT. To test for Cu^{II} binding, MmoS was diluted to 30 μM with chelexed ddH₂O and dialyzed against 500 mL of 50 mM Tris (pH 7.2, 7.4, or 8.0), 0.5 M NaCl, 50–200 μM CuSO₄, and 5% glycerol. Excess copper was removed by further dialysis against the same buffer lacking CuSO₄. To test for Cu^I binding, the same protocol was used, with 50–200 μM CuCl₂ and 1–10 mM ascorbic acid. For each experiment, lysozyme was used as a negative control and was subjected to the same dialysis procedure.

Binding of Cu^I was also investigated in a room-temperature Coy anaerobic chamber. All buffers were degassed prior to introduction into the anaerobic chamber. A stock solution of 36.7 mM CuCl, 10 mM HCl, and 1 M NaCl was prepared, and 1.2 molar equiv of Cu^I was added to 30 μM MmoS that had been dialyzed extensively in the chamber to remove any nonspecifically bound metal ions. Any excess Cu^I was then removed by two additional rounds of dialysis. The human copper chaperone protein Atox1 (20) was used as a positive control to verify the anaerobic Cu^I-loading procedure. The copper contents of MmoS, lysozyme, and Atox1 were measured using a Perkin–Elmer AAnalyst 700 atomic absorption spectrometer with a graphite furnace. The MmoS concentration was determined by UV spectroscopy using the predicted extinction coefficient of $\epsilon_{280} = 86\,000\text{ M}^{-1}\text{ cm}^{-1}$ (21). The protein concentrations of lysozyme and Atox1 were measured using known extinction coefficients at 280 nm.

Flavin Analysis. The MmoS flavin was identified by optical spectroscopy, fluorescence spectroscopy, high-performance liquid chromatography (HPLC) analysis, and mass spectrometry. Optical spectra were recorded using an HP 8452A diode-array spectrometer. Fluorescence spectra were recorded using an ISS PC1 fluorimeter. Samples for fluorescence measurements were dialyzed against 50 mM Tris (pH 8.0) containing 5% glycerol. Aliquots (~3 mg/mL) were then boiled at 95 °C for 10 min, cooled on ice, and centrifuged at 20800g for 10 min at 4 °C to release the flavin. The supernatants were transferred to foil-covered cuvettes. Fluorescence emission spectra were acquired from 480 to 620 nm with an excitation wavelength of 470 nm. Excitation and emission slits were both set at 4 nm. To distinguish between FAD and flavin mononucleotide (FMN), phosphodiesterase I (3 milliunits/ μL) from *Crotalus adamanteus* venom (Sigma) was added (19–950 μL sample) and the emission spectrum was recorded again (22, 23).

For HPLC analysis, MmoS was heat-denatured for 15 min at 95 °C in the dark and the flavin was isolated by filtration and centrifugation at 20800g for 20 min at 4 °C. A Bio-Sil Sec-125 gel-filtration HPLC column (Bio-Rad, 300 \times 78 mm) was equilibrated with 50 mM Tris (pH 7.2), 0.5 M urea, and 10% glycerol with a flow rate of 1.0 mL/min. The column was calibrated with different concentrations of FMN and FAD standards (0.1, 0.5, and 1.0 μM , Sigma). Flavin

isolated from MmoS was applied to the column, eluted using the same buffer, exchanged into acetonitrile, and lyophilized. The lyophilized MmoS flavin as well as the FAD and FMN standards were further analyzed by electrospray ionization mass spectrometry (ESI–MS). To avoid photoconversion of FAD to FMN, flavin samples were kept in the dark at all times. The extinction coefficient at 450 nm for MmoS-bound FAD ($16\,505\text{ M}^{-1}\text{ cm}^{-1}$) was calculated on the basis of that of free FAD ($11\,400\text{ M}^{-1}\text{ cm}^{-1}$) and the ratio of A_{450} values for FAD bound to MmoS and FAD released from MmoS (22).

Determination of the Redox Potential of MmoS-Bound FAD. The redox potential of the MmoS FAD was determined as described by Massey (24). A 500 μL solution of 10–46 μM MmoS in 50 mM Tris (pH 8.0) and 5% glycerol was incubated anaerobically at 25 °C in a customized tonometer with 5 μM phenosafranin as a redox indicator and 2 μM benzyl viologen as a redox mediator. Anaerobiosis was established by flushing the tonometer with nitrogen in a Coy anaerobic chamber. A stock solution of 5–20 mM sodium dithionite was added in 5 μL aliquots using a 250 μL Hamilton syringe with a repeating dispenser. Prior to reduction with dithionite, the solution was equilibrated for 30 min to 1 h. The concentrations of oxidized and reduced MmoS-bound FAD and phenosafranin were measured after each dithionite addition by monitoring the absorbances of FAD at 450 nm and phenosafranin at 522 nm using a HP 8452A diode-array spectrometer. The redox potential was determined by plotting log(ox/red) phenosafranin versus log-(ox/red) MmoS–FAD according to the method of Minnaert (25).

RESULTS

MmoS Purification and Oligomerization State. The MmoS construct was designed to include residues 85–1178 because residues 19–41 are predicted to form a transmembrane domain and residues 42–84 do not correspond to any known domains and could be unstructured. Optimized expression and purification via nickel-affinity and gel-filtration chromatography resulted in a clean preparation of the MmoS protein (Figure 2). During purification, the MmoS-containing fractions are bright yellow in color, suggesting the presence of a cofactor. The typical yield of purified MmoS is ~2 mg/L cell culture. The oligomerization state of MmoS was determined by calibrated gel-filtration chromatography (Figure 3). The theoretical molecular mass of the N-terminally truncated MmoS based on its protein sequence is 120 kDa. MmoS eluted significantly after the void volume and thyroglobulin (669 kDa) but right before ferritin (440 kDa) (inset of Figure 3). The molecular weight was calculated to be 480 kDa, corresponding to a tetramer. Notably, NifL, the sensor protein in the nitrogenase two-component system, is also a tetramer (26, 27). Other PAS domain-containing proteins, including the transcription factor PpsR, which is involved in the expression of photosystem genes (28), have been reported to form tetramers as well.

Copper-Binding Studies. To investigate whether MmoS senses copper directly, both in vivo and in vitro Cu^I- and Cu^{II}-loading protocols were employed. First, Cu^{II} was added to cells at the time of MmoS induction, a procedure that has been successful for various copper-trafficking proteins (29,

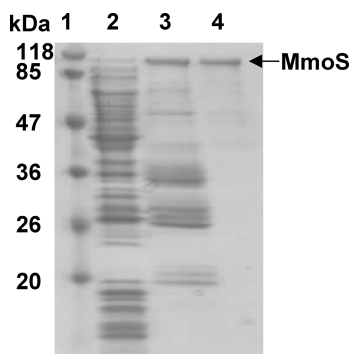


FIGURE 2: SDS-PAGE 15% acrylamide gel of MmoS (120 kDa) purification. Lane 1, molecular-mass standards; lane 2, crude cell extract; lane 3, MmoS-containing fraction after nickel-affinity chromatography on chelating Sepharose; and lane 4, purified MmoS after gel filtration on Superdex 200. MmoS migrates closer to 100 kDa, although the predicted molecular mass is 120 kDa.

30). MmoS purified from these cells contained <0.1 copper ion per MmoS monomer, as measured by atomic absorption spectroscopy. Dialysis versus buffers containing Cu^{I} /ascorbate or Cu^{II} at several pH conditions did not result in specific copper binding to MmoS nor did the anaerobic addition of Cu^{I} . Similar results were obtained for lysozyme, which does not bind copper and served as a negative control. As a positive control, the anaerobic Cu^{I} -loading procedure was performed in parallel for the copper chaperone Atox1 and resulted in 0.6 Cu^{I} ions per monomer, a value consistent with the copper-bridged dimer observed crystallographically (31). On the basis of these data, MmoS is not a copper-binding protein.

Identification of the Flavin. Purified MmoS is bright yellow in color, suggesting the presence of a cofactor. The optical spectrum exhibits peaks at 376 and 444 nm, indicative of an oxidized flavin (Figure 4) (32). Fluorescence emission spectra and phosphodiesterase treatment were used to identify the flavin. This assay exploits the fact that the fluorescence

emission of FMN is 10-fold higher than that of FAD (22). If treatment with phosphodiesterase, which catalyzes the conversion of FAD to FMN and AMP, results in a significant increase in fluorescence, then FAD is present. If no increase in fluorescence is observed, then FMN is likely present (22, 23). The fluorescence emission of MmoS increased by ~ 17 -fold upon phosphodiesterase treatment (Figure 5A), suggesting that MmoS binds FAD. Similar results were obtained from the sensor domain, establishing that the FAD binds within the N-terminal PAS-PAC domain-containing region of MmoS. The identity of the flavin was additionally confirmed by gel-filtration HPLC. The isolated flavin had the same retention time as the FAD standard, eluting prior to the FMN standard (Figure 5B). Finally, ESI-MS analysis indicated the presence of FAD (data not shown). Using the theoretical extinction coefficient of $16\,505\text{ M}^{-1}\text{ cm}^{-1}$ for MmoS-bound FAD, the stoichiometry is 0.93 ± 0.06 mol of FAD/mol of MmoS.

Redox Potential of MmoS-Bound FAD. The redox potential of the MmoS FAD was measured by chemical reduction in the presence of a redox-sensitive dye (24, 33). MmoS was reduced by the addition of dithionite, and phenosafranin ($E_0 = -282\text{ mV}$ at pH 8.0) was used as the reference dye. The reduction of MmoS-bound FAD and phenosafranin was monitored by the decreases in absorbance at 450 and 522 nm, respectively. The redox potential of MmoS-bound FAD was obtained by calculating the concentrations of oxidized and reduced MmoS-FAD and phenosafranin after each dithionite addition. The $\log(\text{ox/red})$ phenosafranin versus $\log(\text{ox/red})$ MmoS-FAD was plotted according to Minnaert, and the redox potential of MmoS-FAD was determined from the y-axis intercept, where $\log(\text{ox/red})$ phenosafranin equals 0 (25). On the basis of three independent experiments, the redox potential of MmoS-FAD is $-290 \pm 2\text{ mV}$ at pH 8.0 and 25°C (Figure 6).

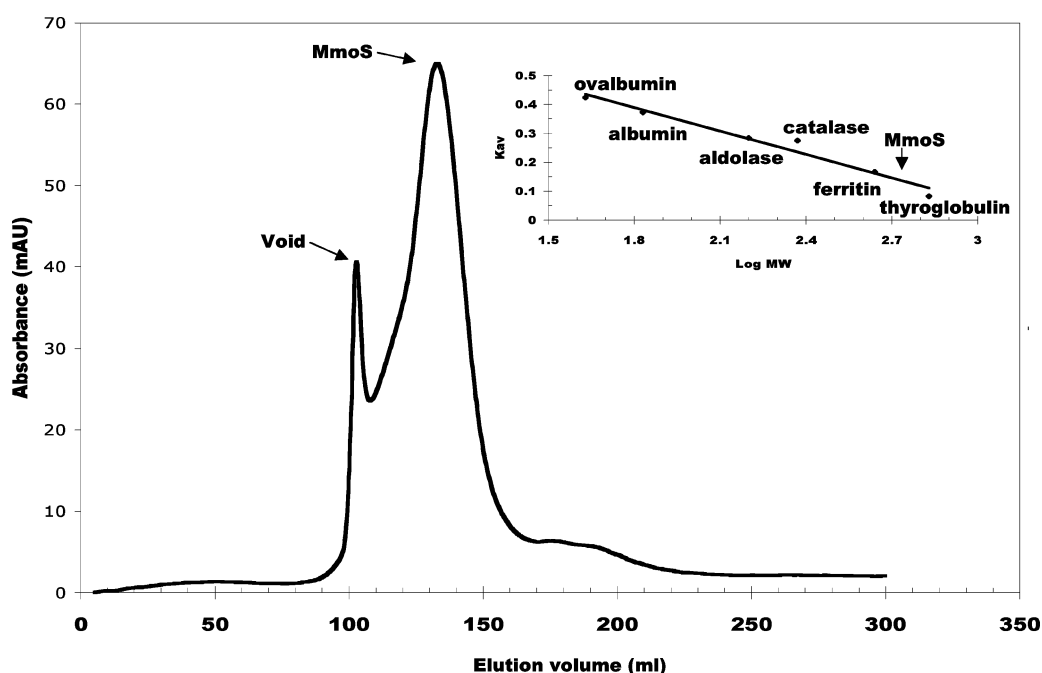


FIGURE 3: Oligomeric state of MmoS determined by gel filtration on Sephacryl S-300. (Inset) Plot of K_{av} as a function of $\log(\text{molecular weight})$. MmoS elutes after thyroglobulin (669 kDa) and before ferritin (440 kDa).

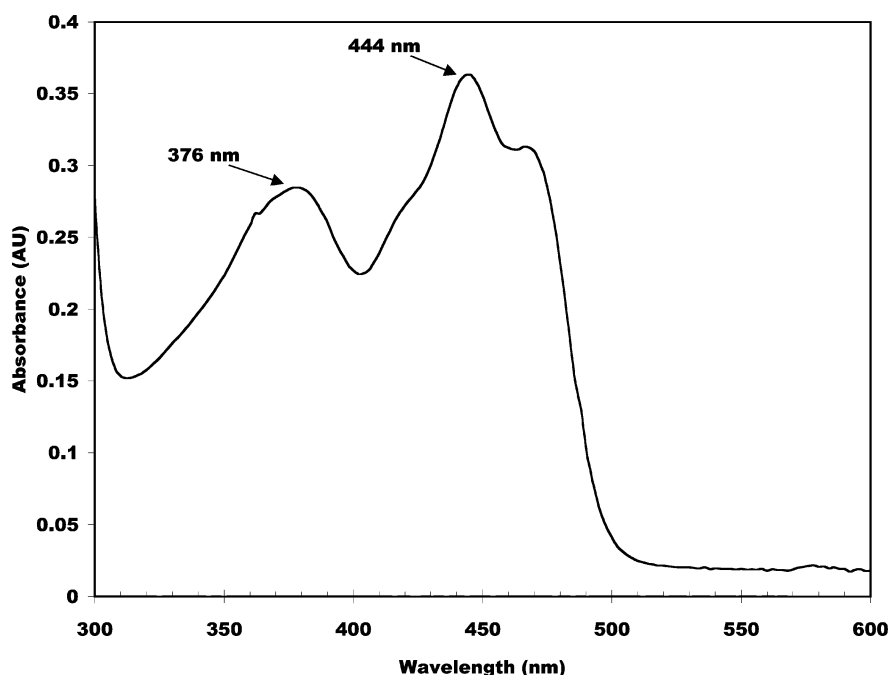


FIGURE 4: Optical spectrum of MmoS [2.5 mg/mL in 50 mM Tris (pH 8.0), 0.5 M NaCl, and 10% glycerol]. The peaks at 376 and 444 nm are characteristic of an oxidized flavin.

DISCUSSION

The *M. capsulatus* (Bath) MmoS protein has been proposed to function as the sensor component of a two-component signaling system involved in copper-dependent expression of sMMO (10). The sensing mechanism has not been elucidated. Extensive efforts to load MmoS with Cu^{I} and Cu^{II} were unsuccessful, indicating that MmoS may not sense copper directly. The possibility that the N-terminal 84 residues contain a copper-binding site cannot be eliminated but is unlikely based on the sequence. The N-terminal periplasmic 18 residues include one methionine in addition to the N-terminal methionine, and the 43 residues following the transmembrane region contain one methionine. The predicted transmembrane helix does include a cysteine, methionine, and histidine, but these residues could not form a metal-binding site within the geometrical constraints of an α helix.

Each monomer in the MmoS tetramer contains one molecule of FAD bound to the N-terminal PAS–PAC domains. The presence of FAD in MmoS distinguishes it from other sensor components that respond to metal-ion concentrations. The PhoP–PhoQ and PmrA–PmrB systems in *Salmonella* and other microorganisms respond to Mg^{II} and Fe^{III} , respectively (34). The PcoR–PcoS (35), CopR–CopS (36), and CusR–CusS (37) two-component systems regulate the expression of copper-resistant genes in bacteria. Similar systems exist for Ag^{I} (38) and $\text{Co}^{\text{II}}/\text{Zn}^{\text{II}}/\text{Cd}^{\text{II}}$ (39). It is not known whether these sensor proteins bind metal ions directly, although a periplasmic HExxE motif has been implicated in Fe^{III} binding by PmrB (40). All of these sensor components are smaller than MmoS and do not contain any predicted PAS–PAC domains, suggesting that a flavin cofactor is probably not present. Thus, the sensing mechanism is not likely to be the same as that employed by MmoS.

There are several examples of FAD-containing sensor proteins in two-component systems, however. NifL from the diazotrophic bacteria *Azotobacter vinelandii* (26) and *Kleb-*

siella pneumoniae (41) bind FAD via a PAS domain. In response to oxygen or fixed nitrogen, NifL inhibits the ability of the NifA protein to activate the transcription of genes involved in nitrogenase biosynthesis (14, 42). Redox sensing occurs via the FAD cofactor. When the FAD is oxidized, NifL inhibits NifA, but dithionite reduction reverses the inhibition (26, 27). The physiological electron donor is not known. Although NifL contains a C-terminal histidine kinase domain that binds adenosine nucleotides, autophosphorylation or phosphotransfer activities have not been detected, suggesting that the mechanism of NifA inhibition involves protein–protein interactions (14).

FAD also functions as a redox sensor in the *E. coli* aerotaxis receptor Aer (43, 44). Aerotaxis enables bacteria to actively swim away from hypoxic regions. Aer responds to the cellular redox state rather than sensing oxygen directly. The specific signal is not known but is proposed to derive from the interaction with components of the electron-transport system or diffusible quinone cofactors (44). Although NifL and Aer appear to be most similar to MmoS, there is another subset of PAS domains called light, oxygen, or voltage (LOV) domains that also bind flavins. LOV domains in the phototropins sense blue light with FMN, resulting in phototropism (45). In higher organisms, LOV domains occur in circadian clock proteins such as WC-1, which senses light with FAD (46).

The redox potential of the MmoS-bound FAD is -290 ± 2 mV at pH 8.0 and 25 °C. This value is similar to those reported for *A. vinelandii* NifL (-226 mV at pH 8) (47) and *K. pneumoniae* NifL (-277 ± 5 mV at pH 8) (48). Because MmoS does not bind copper ions and is most similar to flavin-containing redox sensors, the copper switch might involve a redox signal. One possibility is that the oxidation of FADH_2 to FAD is directly coupled to the reduction of aqueous Cu^{II} to Cu^{I} ($E_0 = 150$ mV). However, some methanotrophs are believed to acquire copper via methanobactin, a siderophore-like Cu^{I} chelator (49, 50), and therefore,

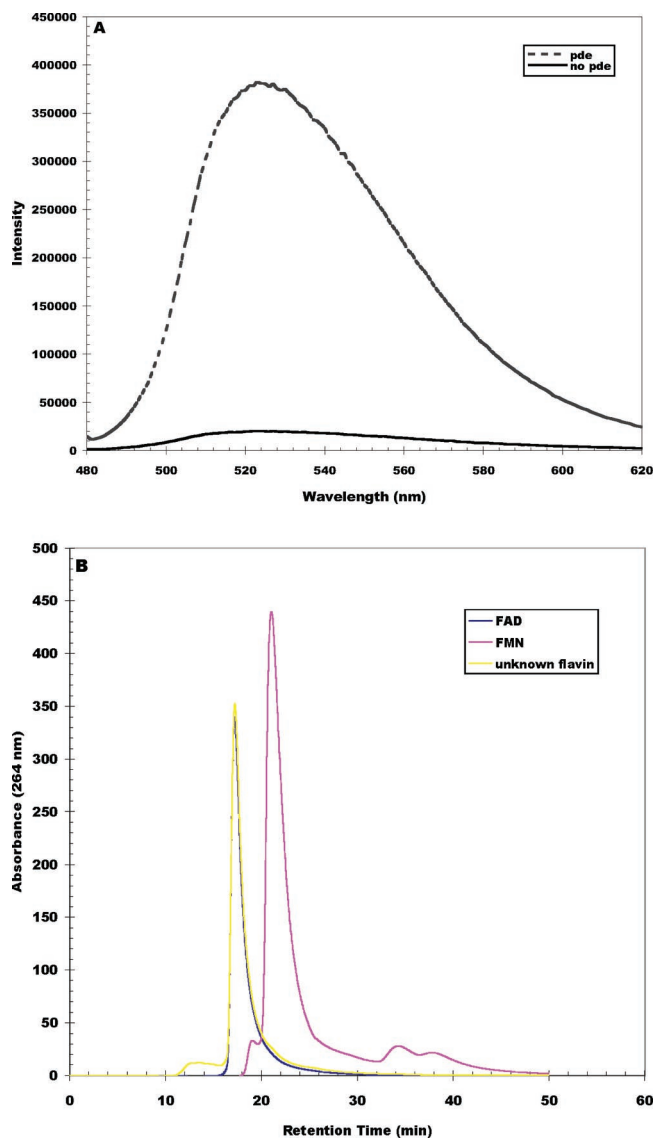


FIGURE 5: Identification of MmoS flavin. (A) Fluorescence emission spectra before (—) and after (---) phosphodiesterase (pde) treatment. (B) HPLC traces of FAD and FMN standards and MmoS flavin.

copper in the cytoplasm is likely to be Cu^{I} rather than Cu^{II} . It is currently not known whether methanobactin plays a role in the copper-sensing mechanism. Reduction of FAD to FADH_2 could also be coupled to oxidation of protein- or methanobactin-bound Cu^{I} . It is well known that a protein environment can significantly affect the potential of bound copper ions (51). Alternatively, additional factors, such as proteins or diffusible small molecules like quinones, could be affected by copper levels and then mediate a redox change at the MmoS FAD site. Finally, reactive oxygen species generated by copper could generate the signal.

A reasonable hypothesis is that the MmoS FAD cofactor exists at low copper levels in the reduced FADH_2 state, perhaps aided by a flavin reductase (Figure 7A). This form of MmoS autophosphorylates a histidine residue and transfers the phosphate to MmoQ. As proposed by Murrell and co-workers, MmoQ then interacts with MmoR, which activates the transcription of the sMMO genes (10). When copper levels increase, the oxidation of FADH_2 to FAD causes a conformational change in MmoS, promoting an interaction with MmoR (Figure 7B). Analogous to the NifL–NifA

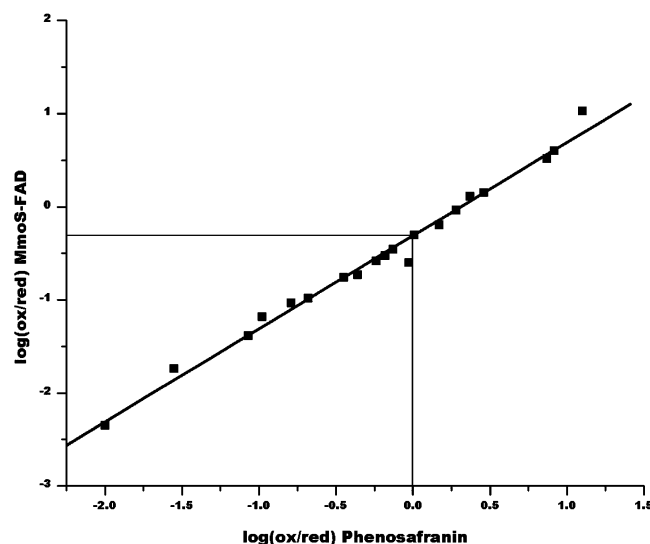


FIGURE 6: Representative Nernst plot of $\log(\text{ox/red})$ phenosafranin as a function of $\log(\text{ox/red})$ MmoS–FAD. The redox potential of MmoS–FAD was obtained from the y intercept, where $\log(\text{ox/red})$ phenosafranin equals 0. Using the midpoint potential of phenosafranin $E_0 = -282$ mV at pH 8.0, E_0 of MmoS–FAD is -282 mV + $(-0.306 \times 30$ mV) = -291.2 mV.

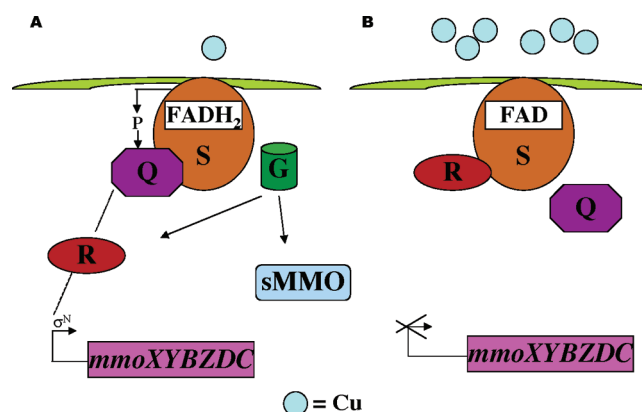


FIGURE 7: Model for the regulation of sMMO expression. (A) Low copper levels. (B) High copper levels.

system, the interaction between MmoS and MmoR inhibits the ability of MmoR to activate transcription. Further biochemical and genetic studies of MmoS, MmoQ, and MmoR are critical to testing this model.

ACKNOWLEDGMENT

We thank M. Sazinsky and G. Gassner for helpful discussions.

REFERENCES

- Hanson, R. S., and Hanson, T. E. (1996) Methanotrophic bacteria, *Microbiol. Rev.* 60, 439–471.
- Lieberman, R. L., and Rosenzweig, A. C. (2004) Biological methane oxidation: Regulation, biochemistry, and active site structure of particulate methane monooxygenase, *Crit. Rev. Biochem. Mol. Biol.* 39, 147–164.
- Merkx, M., Kopp, D. A., Sazinsky, M. H., Blazyk, J. L., Müller, J., and Lippard, S. J. (2001) Dioxygen activation and methane hydroxylation by soluble methane monooxygenase: A tale of two irons and three proteins, *Angew. Chem., Int. Ed.* 40, 2782–2807.
- Stanley, S. H., Prior, S. D., Leak, D. J., and Dalton, H. (1983) Copper stress underlies the fundamental change in intracellular location of methane monooxygenase in methane oxidizing organisms: Studies in batch and continuous cultures, *Biotechnol. Lett.* 5, 487–492.

5. Prior, S. D., and Dalton, H. (1985) The effect of copper ions on membrane content and methane monooxygenase activity in methanol-grown cells of *Methylococcus capsulatus* (Bath), *J. Gen. Microbiol.* **131**, 155–163.
6. Murrell, J. C., McDonald, I. R., and Gilbert, B. (2000) Regulation of expression of methane monooxygenases by copper ions, *Trends Microbiol.* **8**, 221–225.
7. Burrows, K. J., Cornish, A., Scott, D., and Higgins, I. J. (1984) Substrate specificities of the soluble and particulate methane monooxygenases of *Methylosinus trichosporium* OB3b, *J. Gen. Microbiol.* **130**, 327–333.
8. Sullivan, J. P., Dickinson, D., and Chase, C. A. (1998) Methanotrophs, *Methylosinus trichosporium* OB3b, sMMO, and their application to bioremediation, *Crit. Rev. Microbiol.* **24**, 335–373.
9. Phelps, P. A., Agarwal, S. K., Speitel, G. E., Jr., and Georgiou, G. (1992) *Methylosinus trichosporium* OB3b mutants having constitutive expression of soluble methane monooxygenase in the presence of high levels of copper, *Appl. Environ. Microbiol.* **58**, 3701–3708.
10. Csáki, R., Bodrossy, L., Klem, J., Murrell, J. C., and Kovács, K. L. (2003) Genes involved in the copper-dependent regulation of soluble methane monooxygenase of *Methylococcus capsulatus* (Bath): Cloning, sequencing and mutational analysis, *Microbiology* **149**, 1785–1795.
11. Stafford, G. P., Scanlan, J., McDonald, I. R., and Murrell, J. C. (2003) *rpoN*, *mmoR* and *mmoG*, genes involved in regulating the expression of soluble methane monooxygenase from *Methylosinus trichosporium* OB3b, *Microbiology* **149**, 1771–1784.
12. Stock, A. M., Robinson, V. L., and Goudreau, P. N. (2000) Two-component signal transduction, *Annu. Rev. Biochem.* **69**, 183–215.
13. West, A. H., and Stock, A. M. (2001) Histidine kinases and response regulator proteins in two-component signaling systems, *Trends Biochem. Sci.* **26**, 369–376.
14. Martinez-Argudo, I., Little, R., Shearer, N., Johnson, P., and Dixon, R. (2004) The NifL–NifA system: A multidomain transcriptional regulatory complex that integrates environmental signals, *J. Bacteriol.* **186**, 601–610.
15. Baker, M. D., Wolanin, P. M., and Stock, J. B. (2006) Signal transduction in bacterial chemotaxis, *BioEssays* **28**, 9–22.
16. Letunic, I., Copley, R. R., Pils, B., Pinkert, S., Schultz, J., and Bork, P. (2006) SMART 5: Domains in the context of genomes and networks, *Nucleic Acids Res.* **34**, D257–D260.
17. Hefti, M., François, K.-J., de Vries, L. C., Dixon, R., and Vervoort, J. (2004) The PAS fold: A redefinition of the PAS domain based upon structural prediction, *Eur. J. Biochem.* **271**, 1198–1208.
18. Taylor, B. L., and Zhulin, I. B. (1999) PAS domains: Internal sensors of oxygen, redox potential, and light, *Microbiol. Mol. Biol. Rev.* **63**, 479–506.
19. Aravind, L., and Ponting, C. P. (1997) The GAF domain: An evolutionary link between diverse phototransducing proteins, *Trends Biochem. Sci.* **22**, 458–459.
20. Wernimont, A. K., Yatsunyk, L. A., and Rosenzweig, A. C. (2004) Binding of copper(I) to the Wilson disease protein and its copper chaperone, *J. Biol. Chem.* **279**, 12269–12276.
21. Gill, S. G., and von Hippel, P. H. (1989) Calculation of protein extinction coefficients from amino acid sequence data, *Anal. Biochem.* **182**, 319–326.
22. Aliverti, A., Curti, B., and Vanoni, M. A. (1999) Identifying and quantitating FAD and FMN in simple and in iron–sulfur-containing flavoproteins, in *Methods in Molecular Biology: Flavoprotein Protocols* (Chapman, S. K., and Reid, G. A., Eds.) pp 9–23, Humana Press, Totowa, NJ.
23. Forti, G., and Sturani, E. (1968) On the structure and function of reduced nicotinamide adenine dinucleotide phosphate–cytochrome *f* reductase of spinach chloroplasts, *Eur. J. Biochem.* **3**, 461–472.
24. Massey, V. (1991) A simple method for the determination of redox potentials, in *Flavin and Flavoproteins* (Curti, B., Ronchi, S., and Zanetti, G., Eds.) pp 59–66, Walter de Gruyter, Como, Italy.
25. Minnaert, K. (1965) Measurement of the equilibrium constant of the reaction between cytochrome *c* and cytochrome *a*, *Biochim. Biophys. Acta* **110**, 42–56.
26. Hill, S., Austin, S., Eydmann, T., Jones, T., and Dixon, R. (1996) *Azotobacter vinelandii* NifL is a flavoprotein that modulates transcriptional activation of nitrogen-fixation genes via a redox-sensitive switch, *Proc. Natl. Acad. Sci. U.S.A.* **93**, 2143–2148.
27. Söderbäck, E., Reyes-Ramirez, F., Eydmann, T., Austin, S., Hill, S., and Dixon, R. (1998) The redox- and fixed nitrogen-responsive regulatory protein NifL from *Azotobacter vinelandii* comprises discrete flavin and nucleotide-binding domains, *Mol. Microbiol.* **28**, 179–192.
28. Gomelsky, M., Horne, I. M., Lee, H. J., Pemberton, J. M., McEwan, A. G., and Kaplan, S. (2000) Domain structure, oligomeric state, and mutational analysis of PpsR, the *Rhodospirillum rubrum* repressor of photosystem gene expression, *J. Bacteriol.* **182**, 2253–2261.
29. Heaton, D. N., George, G. N., Garrison, G., and Winge, D. R. (2001) The mitochondrial copper metallochaperone Cox17 exists as an oligomeric, polycopper complex, *Biochemistry* **40**, 743–751.
30. Lutsenko, S., Petrukhin, K., Cooper, M. J., Gilliam, C. T., and Kaplan, J. H. (1997) N-Terminal domains of human copper-transporting adenosine triphosphatases (the Wilson's and Menkes disease proteins) bind copper selectively *in vivo* and *in vitro* with stoichiometry of one copper per metal-binding repeat, *J. Biol. Chem.* **272**, 18939–18944.
31. Wernimont, A. K., Huffman, D. L., Lamb, A. L., O'Halloran, T. V., and Rosenzweig, A. C. (2000) Structural basis for copper transfer by the metallochaperone for the Menkes/Wilson disease proteins, *Nat. Struct. Biol.* **7**, 766–771.
32. Macheroux, P. (1999) UV–visible spectroscopy as a tool to study flavoproteins, in *Methods in Molecular Biology: Flavoprotein Protocols* (Chapman, S. K., and Reid, G. A., Eds.) pp 1–7, Humana Press, Totowa, NJ.
33. Mayhew, S. G. (1999) Potentiometric measurement of oxidation–reduction potentials, in *Methods in Molecular Biology: Flavoprotein Protocols* (Chapman, S. K., and Reid, G. A., Eds.) pp 49–59, Humana Press, Totowa, NJ.
34. Groisman, E. A. (2001) The pleiotropic two-component regulatory system PhoP–PhoQ, *J. Bacteriol.* **183**, 1835–1842.
35. Brown, N. L., Barrett, S. R., Camakaris, J., Lee, B. T. O., and Rouch, D. A. (1995) Molecular genetics and transport analysis of the copper-resistance determinant (*pco*) from *Escherichia coli* plasmid pRJ1004, *Mol. Microbiol.* **17**, 1153–1166.
36. Mills, S. D., Jasalovich, C. A., and Cooksey, D. A. (1993) A two-component regulatory system required for copper-inducible expression of the copper resistance operon of *Pseudomonas syringae*, *J. Bacteriol.* **175**, 1656–1664.
37. Munson, G. P., Lam, D. L., Outten, F. W., and O'Halloran, T. V. (2000) Identification of a copper-responsive two-component system on the chromosome of *Escherichia coli* K-12, *J. Bacteriol.* **182**, 5864–5871.
38. Gupta, A., Matsui, K., Lo, J. F., and Silver, S. (1999) Molecular basis for resistance to silver cations in *Salmonella*, *Nat. Med.* **5**, 183–188.
39. Perron, K., Caille, O., Rossier, C., van Delden, C., Dumas, J. L., and Kohler, T. (2004) CzcR–CzcS, a two-component system involved in heavy metal and carbapenem resistance in *Pseudomonas aeruginosa*, *J. Biol. Chem.* **279**, 8761–8768.
40. Wösten, M. M. S. M., Kox, L. F. F., Chamnongpol, S., Soncini, F. C., and Groisman, E. A. (2000) A signal transduction system that responds to extracellular iron, *Cell* **103**, 113–115.
41. Schmitz, R. A. (1997) NifL of *Klebsiella pneumoniae* carries an N-terminally bound FAD cofactor, which is not directly required for the inhibitory function of NifL, *FEMS Microbiol. Lett.* **157**, 313–318.
42. Dixon, R. (1998) The oxygen-responsive NifL–NifA complex: A novel two-component regulatory system controlling nitrogenase synthesis in γ -proteobacteria, *Arch. Microbiol.* **169**, 371–380.
43. Bibikov, S. I., Barnes, L. A., Gitin, Y., and Parkinson, J. S. (2000) Domain organization and flavin adenine dinucleotide-binding determinants in the aerotaxis signal transducer Aer of *Escherichia coli*, *Proc. Natl. Acad. Sci. U.S.A.* **97**, 5830–5835.
44. Taylor, B. L., Rebbapragada, A., and Johnson, M. S. (2001) The FAD–PAS domain as a sensor for behavioral responses in *Escherichia coli*, *Antioxid. Redox Signaling* **3**, 867–879.
45. Crosson, S., Rajagopal, S., and Moffat, K. (2003) The LOV domain family: Photoresponsive signaling modules coupled to diverse output domains, *Biochemistry* **42**, 2–10.
46. He, Q., Cheng, P., Yang, Y., Wang, L., Gardner, K. H., and Liu, Y. (2002) White collar-1, a DNA binding transcription factor and a light sensor, *Science* **297**, 840–843.
47. Macheroux, P., Hill, S., Austin, S., Eydmann, T., Jones, T., Kim, S.-O., Poole, R., and Dixon, R. (1998) Electron donation to the flavoprotein NifL, a redox-sensing transcriptional regulator, *Biochem. J.* **332**, 413–419.

48. Klopprogge, K., and Schmitz, R. A. (1999) NifL of *Klebsiella pneumoniae*: Redox characterization in relation to the nitrogen source, *Biochim. Biophys. Acta* 1431, 462–470.
49. Hakemian, A. S., Tinberg, C. E., Kondapalli, K. C., Telser, J., Hoffman, B. M., Stemmler, T. L., and Rosenzweig, A. C. (2005) The copper chelator methanobactin from *Methylosinus trichosporium* OB3b binds Cu(I), *J. Am. Chem. Soc.* 127, 17142–17143.
50. Kim, H. J., Galeva, N., Larive, C. K., Alterman, M., and Graham, D. W. (2005) Purification and physical-chemical properties of methanobactin: A chalkophore from *Methylosinus trichosporium* OB3b, *Biochemistry* 44, 5140–5148.
51. Solomon, E. I., Szilagyi, R. K., George, S. D., and Basumallick, L. (2004) Electronic structures of metal sites in proteins and models: Contributions to function in blue copper proteins, *Chem. Rev.* 104, 419–458.

BI060693H